A caudorostral wave of RALDH2 conveys anteroposterior information to the cardiac field

Tatiana Hochgreb[1,*], Vania L. Linhares[1,2,*], Diego C. Menezes[1], Allysson C. Sampaio[1], Chao Y. I. Yan[3], Wellington V. Cardoso[4], Nadia Rosenthal[5] and José Xavier-Neto[1,†]

[1]Laboratório de Genética e Cardiologia Molecular InCor – HC.FMUSP 05403-900 São Paulo-SP, Brazil
[2]Laboratório de Cardiologia Celular e Molecular IBCCF-UFRJ Rio de Janeiro-RJ, Brazil
[3]Departamento de Histologia e Embriologia, ICB-USP, São Paulo-SP, Brazil
[4]Pulmonary Center – Boston University School of Medicine, Boston, MA, USA
[5]EMBL European Molecular Biology Laboratory Mouse Biology Programme, Monterotondo-Scalo, Italy

*These authors contributed equally to this work
†Author for correspondence (e-mail: xavier.neto@incor.usp.br)

Accepted 9 July 2003

Development 130, 5363-5374

doi:10.1242/dev.00750

Summary

Establishment of anteroposterior (AP) polarity is one of the earliest decisions in cardiogenesis and plays an important role in the coupling between heart and blood vessels. Recent research implicated retinoic acid (RA) in the communication of AP polarity to the heart. We utilized embryo culture, in situ hybridization, morphometry, fate mapping and treatment with the RA pan-antagonist BMS493 to investigate the relationship between cardiac precursors and RA signalling. We describe two phases of AP signalling by RA, reflected in RALDH2 expression. The first phase (HH4-7) is characterized by increasing proximity between sino-atrial precursors and the lateral mesoderm expressing RALDH2. In this phase, RA signalling is consistent with diffusion of the morphogen from a large field rather than a single hot spot. The second phase (HH7-8) is characterized by progressive encircling of cardiac precursors by a field of RALDH2 originating from a dynamic and evolutionary-conserved caudorostral wave pattern in the lateral mesoderm. At this phase, cardiac AP patterning by RA is consistent with localized action of RA by regulated activation of the *Raldh2* gene within an embryonic domain. Systemic treatment with BMS493 altered the cardiac fate map such that ventricular precursors were found in areas normally devoid of them. Topical application of BMS493 inhibited atrial differentiation in left anterior lateral mesoderm. Identification of the caudorostral wave of RALDH2 as the endogenous source of RA establishing cardiac AP fates provides a useful model to approach the mechanisms whereby the vertebrate embryo confers axial information on its organs.

Supplemental data available online

Key words: Heart, Atrium, Ventricle, RALDH2, Retinoic acid, AMHC1, BMS493, Mouse, Chicken, Embryo

Introduction

Establishment of the circulation is a two-pronged process. First, common progenitors form blood vessels and blood cells. Shortly after that, cells in the lateral mesoderm differentiate into endocardial and myocardial types that will organize the primitive circulatory pump: the heart tube. It is only after the basic circulatory plan is laid down, with separate conduits to and from tissues, that pumping from the heart is activated. This schedule for formation of the circulatory system places constraints in cardiac morphogenesis because the heart has to develop according to rules set by the pre-existing vascular system. As such, the heart must receive blood at its posterior pole and return it through its anterior pole. This initial distinction between anterior (outflow) and posterior (inflow) extremities is critical for coupling between heart and blood vessels and is later compounded by further division of intervening cardiac tissue into discrete segments, each displaying marked electrophysiological and contractile differences (De Jong et al., 1992). Thus, it is the partition of the heart in the anteroposterior (AP) axis that extracts useful circulatory work from the cardiac musculature, providing the contractile coordination and directional flow required for effective pumping.

Although a few genes have been identified that play a role in chamber formation (Bruneau, 2002), much remains to be known about how information flows from signalling events to the synthesis and assembly of specific contractile and electrophysiological modules along the cardiac AP axis. Recently, much information has been obtained showing that retinoic acid (RA) is a morphogen that communicates AP polarity to the heart (Xavier-Neto et al., 2001). RA is synthesized from vitamin A through a chain of oxidative reactions, from retinol to retinaldehyde and from retinaldehyde to RA. The former reaction is mediated by alcohol dehydrogenases (ADHs) and the latter by retinaldehyde dehydrogenases (RALDHs). Because ADH3 activity is ubiquitous (Molotkov et al., 2002), the availability of RA is dictated by the distribution of RALDHs. Previous studies

indicate that RALDH2 is the main RALDH in early cardiac development (Moss et al., 1998; Niederreither et al., 2001). RALDH2 is expressed in the developing heart to generate sequential programs of RA synthesis in myocardial and epicardial layers (Moss et al., 1998; Xavier-Neto et al., 2000). Using immunohistochemistry we previously showed that *Raldh2* is expressed in a region of the avian lateral mesoderm that contains sino-atrial precursors in HH8 embryos. Moreover, at HH9^{-}, posterior cardiac precursors express *Raldh2* (Xavier-Neto et al., 2000) and *Amhc1*, a marker of commitment to the atrial phenotype (Yutzey et al., 1994). From these stages onwards, *Raldh2* expression remains associated with sino-atrial structures until a myocardial wave takes it to ventricles and conotruncus. This myocardial phase is then replaced by another wave of epicardial RALDH2 that envelops the heart. Thus, these patterns provided clues that RALDH2 plays important roles in sino-atrial morphogenesis, in the development of the coronary circulation and in growth of the ventricular myocardium (Xavier-Neto et al., 2000; Pérez-Pomares et al., 2002; Stuckmann et al., 2003).

The crucial role of RALDH2 in sino-atrial development has been established by pharmacological, genetic and dietary manipulations (Xavier-Neto et al., 1999; Niederreither et al., 1999; Kostetskii et al., 1999). Although effective, these approaches were systemic and protracted, and therefore lacked the spatial and temporal resolution required to define target cell populations and developmental times when the endogenous RA signal polarizes the heart. Thus, to fill these fundamental gaps in our understanding of the developmental mechanisms that communicate and maintain sino-atrial fates, here we describe the changing spatial relationship between cardiac precursors and the domains of *Raldh2* expression during the critical phases of cardiac AP patterning. The different stages of the relationship between cardiac precursors and RALDH2 were correlated to the states of commitment of anterior and posterior cardiac precursors using treatments with RA or with a RA pan-antagonist, respectively. We show that there are two phases of cardiac AP patterning by RA. The first phase, the specification phase (HH5-7), is characterized by increasing proximity between sino-atrial precursors and the anterior margin of the RALDH2-expressing mesoderm. The second phase, the determination phase (HH7-8), is characterized by progressive encircling of sino-atrial precursors by a field of RALDH2 originating from a highly dynamic caudorostral wave in the lateral mesoderm. Integrating the data on morphology, fate mapping and states of commitment we conclude that the RA required for cardiac AP specification is provided by the posterior mesoderm (HH5-7). Later, the RA required for determination of AP fates is provided by the anterior lateral mesoderm (HH7-8) in the form of a caudorostral wave of RALDH2. Identification of the tissue sources of RA that define AP boundaries in cardiac precursors should pave the way to a better understanding of how AP information is relayed to the developing heart.

Materials and methods

Embryos

Fertile unincubated chicken eggs were obtained from commercial sources. Eggs were incubated at 37°C and embryos were harvested at indicated stages. Chicken embryos were harvested and cultured according to Chapman et al. (Chapman et al., 2001). Mouse embryos from the FVB/N strain were collected at 7.5 through 9.5 dpc (days post-coitum). Chicken and mouse embryos were staged according to Hamburger and Hamilton and Downs and Davies, respectively (Hamburger and Hamilton, 1951; Downs and Davies, 1993). Embryos were fixed at 4°C in phosphate buffered saline (PBS) pH 7.4 containing 4% paraformaldehyde, dehydrated and stored in methanol until analysis.

In situ hybridization

In situ hybridization was performed according to Wilkinson (Wilkinson, 1992) using probes against chicken and mouse mRNAs such as chick GATA4 (Jiang et al., 1998), chick RALDH2 (Swindell et al., 1999), AMHC1 (Yutzey et al., 1994), mouse Tbx-5 (Bruneau et al., 1999) and mouse RALDH2 (Zhao et al., 1996). For double in situ hybridization, embryos were treated as described by Stern (Stern, 1998). GATA4 and Tbx-5 were revealed with BMPurple. RALDH2 probes were revealed using BMPurple or INT/BCIP. RALDH2 immunohistochemistry was performed as described (Xavier-Neto et al., 1999). Double mouse Tbx-5 in situ hybridization/β-galactosidase stains in RARE*hsplacZ* embryos (Rossant et al., 1991) were performed according to Houzelstein and Tajbakhsh (Houzelstein and Tajbakhsh, 1999). Paraffin sections were generated according to Sassoon and Rosenthal (Sassoon and Rosenthal, 1993). Isotopic (^{35}S-labeled riboprobes) in situ hybridization was performed on paraffin sections (6-12 μm) as described by Cardoso et al. (Cardoso et al., 1996) and the labelling displayed in pseudocolor.

Image analyses

Embryos and paraffin sections were photographed on stereozoom and fluorescence microscopes. Bright field and fluorescent pictures were taken with a digital camera and acquired with MediaCybernetics software. Images in slides were acquired with a slide scanner and processed with Adobe Photoshop.

Morphometry

Expression patterns from 200 chicken embryos were quantified with the Scion Image program (ported from NIH Image for the Macintosh by Scion Corporation and available on the Internet at http://www.Scioncorp.com). Unprocessed images in TIFF format were fed into Scion to obtain grayscale images that were calibrated to give distances in μm. Grayscale images were submitted to density slicing which segments images on the basis of gray level. By manipulating upper and lower threshold levels in the look up tables, pixels representing low levels of staining were displayed in red, whereas pixels either above (high level of staining) or below threshold (background staining) were unchanged (Fig. 1C-E). Changes in expression patterns were measured as distances from embryonic structures or staining landmarks. We measured four parameters in the lateral mesoderm: (1) Distance traveled by the RALDH2 wave (anterior expansion); (2) Front of the RALDH2 wave (anterior limit of *Raldh2* expression); (3) Anterior limit of the cardiac field (anterior limit of chick *Gata4* expression); (4) Posterior limit of the cardiac field (posterior limit of chick *Gata4* expression).

For embryos at HH5-6, anterior expansion was defined as the distance between the anterior margin of tissue with low intensity of RALDH2 staining and the anterior border of tissue with high level of RALDH2 staining (Fig. 1B,C). For embryos at HH7-10, anterior expansion was defined as the distance between the anterior tip of *Raldh2* expression and a horizontal line transecting the embryo at the boundary between the last formed somite and the unsegmented mesoderm (Fig. 1D,E).

Anterior and posterior limits of chick *Gata4* and chick *Raldh2* expression were measured relative to the anterior tip of Hensen's node. Points above or below it were attributed positive or negative values, respectively. Careful examination of all parameters did not reveal differences between right and left sides. Thus, final averages include both sets of data.

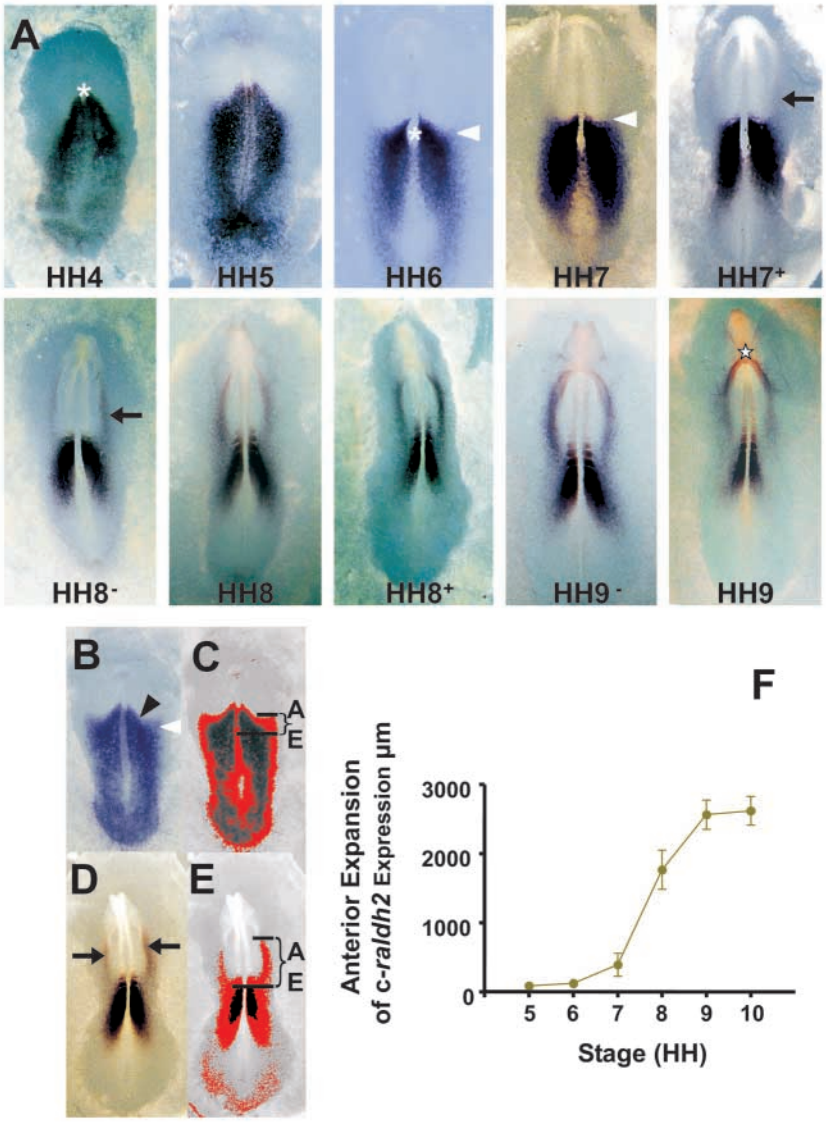

Fig. 1. A caudorostral wave expands RALDH2 anteriorly. (A) In situ hybridization indicates that *Raldh2* is expressed posterior to Hensen's node (*) between HH4-6. At HH6-7 spots of RALDH2 blur the otherwise sharp anteroposterior (AP) boundaries of expression in the lateral mesoderm (white arrowheads). At HH7$^+$ two faint arches of RALDH2 appear in the anterior lateral mesoderm (black arrow). These arches intensify at HH8$^-$-HH8$^+$ and progress anteriorly. At HH9-10 RALDH2 arches join at the midline below the anterior intestinal portal (AIP) (star). (B) HH6. Strong *Raldh2* expression spreads from Hensen's node in a postero-lateral direction (black arrowhead), whereas faint expression appears at the anterior border of the lateral mesoderm (white arrowhead). (C) Grayscale image of B submitted to morphometry. Horizontal bars indicate the limits of high and low *Raldh2* expression and the interval between them defines anterior expansion of RALDH2. (D) HH8$^+$. Strong arches of expression form in the anterior lateral mesoderm (black arrows). (E) Grayscale image of D submitted to morphometry. Upper horizontal bar marks the anterior limit of *Raldh2* expression in the lateral mesoderm. Lower horizontal bar marks the boundary between the last formed somite and the unsegmented paraxial mesoderm. The interval between horizontal bars defines anterior expansion of RALDH2. (F) Expansion of RALDH2 begins slowly between HH6-7 coinciding with appearance of scattered spots of expression at the anterior lateral mesoderm. Expansion reaches maximal rates of development between HH7-8 when faint arches appear at the anterior lateral mesoderm. Thereafter, it tapers off as RALDH2 arches join at midline below the AIP between HH9-10. Data are presented as means±s.e.m. AE, anterior expansion.

Fate mapping

The fluorescent tracer DiI was diluted and loaded into glass pipettes according to Garcia-Martinez and Schoenwolf (Garcia-Martinez and Schoenwolf, 1993). DiI was pressure-injected as a small bolus in the left lateral mesoderm with a Narishige micromanipulator and a Harvard Apparatus picoinjector. After injection embryos were washed in PBS, photographed under fluorescent and bright fields and cultured to HH11$^+$, when they were fixed, examined and photographed again. Injection sites were recorded using grid system and coordinates by Redkar et al. (Redkar et al., 2001). Grids were superimposed on pictures of living HH7 and HH8 embryos. Fluorescence and bright field images were superimposed using Adobe Photoshop. Specific information on each DiI injection point is provided as supplemental data (see Tables S1, S2, S3 at http://dev.biologists.org/supplemental).

We superimposed HH7 and HH8 cardiac fate maps on RALDH2 in situ hybridization pictures from 2 embryos that represented the average patterns determined by morphometric analysis. We adopted the procedure described by Streit to correct for uneven shrinking induced by dehydration and in situ hybridization (Streit, 2002). Corrections were applied by enlarging in situ hybridization pictures of HH7 embryos by 1.0% in the left-right axis and 3.7% in the AP axis. Correction factors for HH8 were 5% and 9%, respectively.

Treatments

Cultured embryos were treated with all-trans RA or the RA pan-antagonist BMS493. Stock solutions of all-trans RA and BMS493 10^{-3} M in DMSO or ethanol, respectively, were diluted in PBS to 10^{-6}, 10^{-5} and 10^{-4} M. Twenty microliters of test solution were applied over embryos beginning at HH4-9. All embryos were harvested at HH10. Controls received vehicle for all-trans RA (DMSO 1% in PBS) or BMS493 (ethanol 10% in PBS). For unilateral treatments of the anterior lateral mesoderm we placed 3 cylinders of agar 1.5% (1.0 mm height, 0.5 mm diameter) (Rugh, 1952) made in PBS containing BMS493 10^{-4} M, on endoderm overlying the left lateral mesoderm between Hensen's node and the headfold. Controls received cylinders containing PBS.

Results

A caudorostral wave of RALDH2

To understand how and when RA affects cardiac precursors we examined the patterns of expression of chick *Raldh2* in the lateral mesoderm of the developing embryo. We established that the early posterior pattern of chick *Raldh2* expression (Swindell et al., 1999) is modified when a caudorostral wave

expands RALDH2 in the anterior lateral mesoderm (Fig. 1A). Anterior expansion of *Raldh2* expression begins at HH6 when the sharp anterior limits of RALDH2 of HH4-5 are blurred by scattered spots of faint RALDH2 staining at the anterior edges of the lateral mesoderm (white arrowheads). At HH7, *Raldh2* expression progresses little beyond the patterns of HH6. However, between stages HH7-8 RALDH2 staining progresses quickly in the anterior direction (black arrows). At HH8^{-} *Raldh2* expression is intensified, but its anterior expansion in the lateral mesoderm slows down. At subsequent stages the bilateral arches of *Raldh2* expression join the midline over the anterior intestinal portal (AIP).

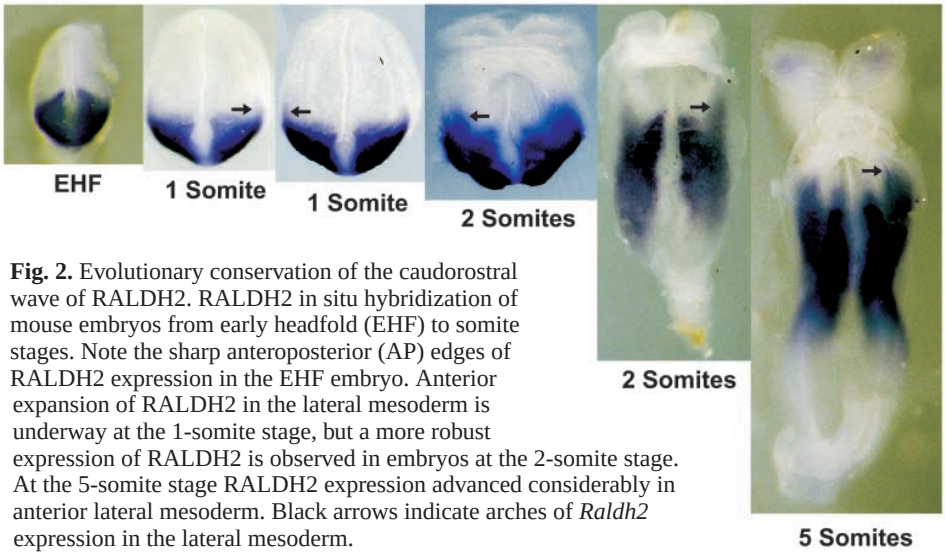

Fig. 2. Evolutionary conservation of the caudorostral wave of RALDH2. RALDH2 in situ hybridization of mouse embryos from early headfold (EHF) to somite stages. Note the sharp anteroposterior (AP) edges of RALDH2 expression in the EHF embryo. Anterior expansion of RALDH2 in the lateral mesoderm is underway at the 1-somite stage, but a more robust expression of RALDH2 is observed in embryos at the 2-somite stage. At the 5-somite stage RALDH2 expression advanced considerably in anterior lateral mesoderm. Black arrows indicate arches of *Raldh2* expression in the lateral mesoderm.

To establish the dynamics of the RALDH2 caudorostral wave in a quantitative fashion we measured the anterior expansion of RALDH2 in the lateral mesoderm (Fig. 1B-E). As shown in Fig. 1F, anterior expansion begins slowly between HH6-7. Between HH7-8, however, it is accelerated to its maximal rate. Thereafter, it proceeds at a much slower pace until bilateral arches of RALDH2 fuse at the midline at HH9-10.

In the mouse embryo, *Raldh2* expression changes are less pronounced than in chicken, but overall, display similar progression. Anterior expansion of RALDH2 in mice begins at the late allantoic bud stage. The maximal rate of anterior expansion occurs between the stages of late headfold and 1 somite (not shown). Thereafter, RALDH2 expansion is slowed between the stages of 1 somite and 2 somites, and, similar to the chicken embryo, its bilateral arches eventually join in the midline over the AIP (Fig. 2 and see RALDH2 whole-mount immunohistochemistry).

Anterior expansion of RALDH2 in the lateral mesoderm conveys RA signalling to cardiac precursors

To gain insight into the role of this RALDH2 caudorostral wave we defined the spatial relationship between cardiac precursors and *Raldh2* expression during the critical phases of cardiac AP differentiation.

We performed in situ hybridization with a chick RALDH2 probe and a chick GATA4 probe as a marker for cardiac precursors. Chick *Gata4* was chosen as a marker because its pattern of expression coincided with the cardiac field as revealed by our fate maps (see *Raldh2* expression and the cardiac fate map). This contrasted with those of chick *nkx-2.5*, which excluded most posterior cardiac precursors (data not shown) (Redkar et al., 2001).

Fig. 3 shows the two phases of the changing relationship between chick GATA4 and chick RALDH2 patterns. The parameters utilized in this morphometric analysis are illustrated in Fig. 3A,B. At HH5 there was a gap of approximately 700 μm separating cardiac precursors from tissue synthesizing RALDH2 (Fig. 3C). This gap narrowed between HH5-7 (Phase 1) and, eventually, RALDH2

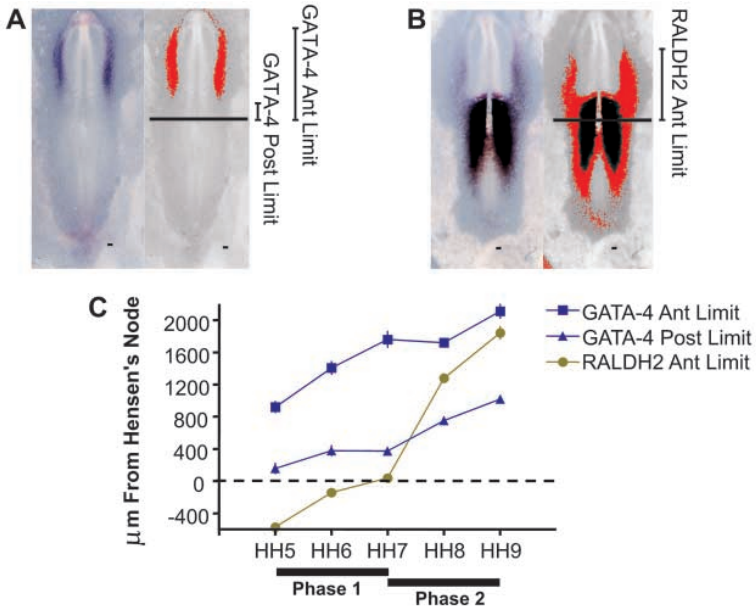

Fig. 3. Two phases of the relationship between RALDH2 and the cardiac field. (A) HH7^{+}. GATA4 in situ hybridization (left) was converted to grayscale image (right) and submitted to morphometry. Anterior and posterior limits of the cardiac field (chick *Gata4* expression) were measured relative to a horizontal bar transecting the anterior tip of Hensen's node. (B) HH7^{+}. RALDH2 in situ hybridization (left) was converted to grayscale image (right) and submitted to morphometry. The anterior limit of RALDH2 expression in the lateral mesoderm was measured relative to the anterior tip of Hensen's node. Chick GATA4 and chick RALDH2 parameters above or below Hensen's node were attributed positive or negative values, respectively. (C) Two phases of cardiac anteroposterior (AP) signalling by RA. Phase 1 is characterized by increasing proximity between RALDH2 and prospective sino-atrial precursors in the posterior extremity of the cardiogenic plate. Phase 2 is characterized by a progressive encircling of sino-atrial precursors in the posterior half of the cardiogenic plate by a field of RALDH2. Data are presented as means±s.e.m.

entered the cardiac field between HH7-8 (Phase 2). At HH8 RALDH2 penetrated deeper into cardiac tissue, overlapping slightly more than the lower half of the cardiac field. At HH9 chick *Raldh2* expression extended over three-quarters of the cardiac field.

Some temporal variation in this sequence was observed in certain embryos. For instance, in some embryos at HH6, the upper limits of chick *Raldh2* and the lower limits of chick *Gata4* were found at approximately 100 μm above Hensen's node. This level of variation suggested that in some embryos chick *Raldh2* expression could reach the cardiac field as soon as HH6. Fig. 4A and Fig. 4B depict embryos displaying such extreme anterior and posterior domains of chick *Raldh2* and chick *Gata4* expression, respectively. In Fig. 4C a double in situ hybridization indicates that extreme anterior and posterior domains of RALDH2 and GATA4 could indeed converge at HH6 to create contact between the cardiac field and the tissue producing RALDH2.

Fig. 4 shows embryos representing the two phases of the changing relationship between chick GATA4 and chick RALDH2 patterns. The double-stained embryo of Fig. 4C represents the extreme point of Phase 1, when chick *Raldh2* expression eventually contacts the most posterior cells of the chick GATA4 domain. Phase 2, represented by Fig. 4D-K, is characterized by progressive overlapping between chick *Gata4* and chick *Raldh2* expression patterns. Alignment of HH8 embryos labeled for chick *Raldh2* or chick *Gata4* shows that these genes display a large area of overlap extending from somites 2-3 almost up to the AIP (Fig. 4D,E). Sections taken through these embryos indicate that chick *Raldh2* and chick *Gata4* are both expressed in the splanchnic mesoderm. Chick *Raldh2* is also expressed in the somatic mesoderm, whereas chick *Gata4* expression also appears in the endoderm (Fig. 4F-I), as previously reported (Kostetskii et al., 1999). RALDH2 and GATA4 isotopic in situ hybridization in consecutive sections confirm that chick *Raldh2* and chick *Gata4* are co-expressed in the splanchnic mesoderm (Fig. 4J and Fig. 4K, respectively).

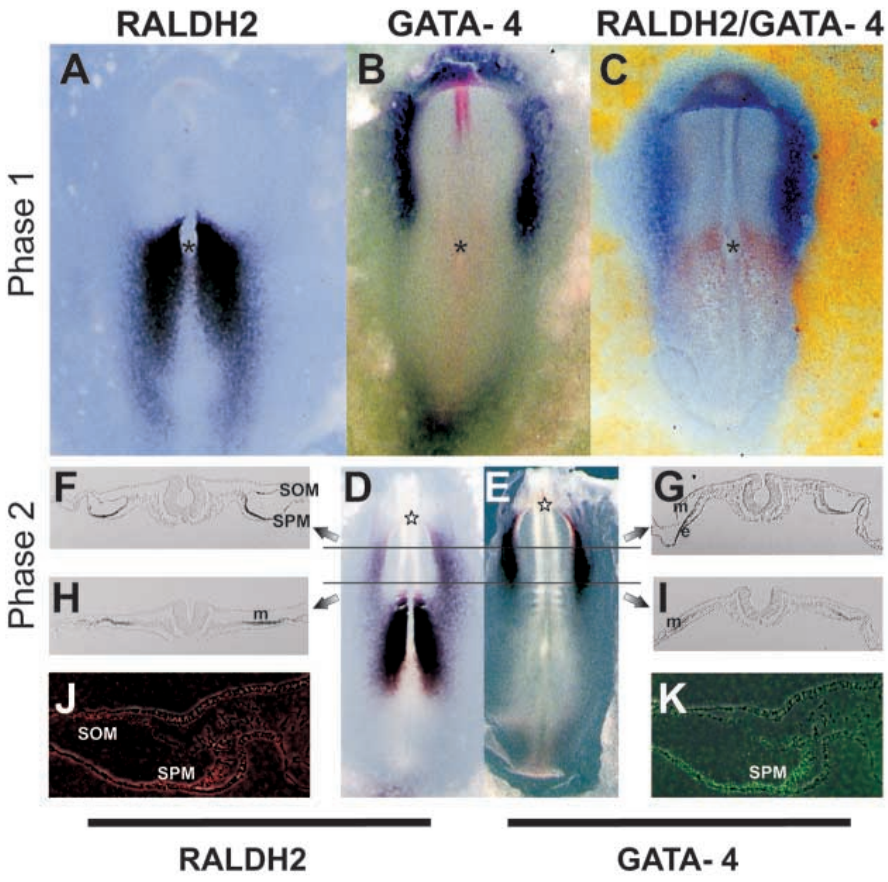

Fig. 4. A caudorostral wave of RALDH2 conveys anteroposterior (AP) information to the cardiac field. (A) HH6 chick RALDH2 in situ hybridization. The anterior limit of chick *Raldh2* expression lies near the anterior tip of Hensen's node. (B) HH6 chick GATA4 in situ hybridization. The posterior limit of chick GATA4 lies near the anterior tip of Hensen's node (star). (C) HH6 double chick RALDH2/chick GATA4 in situ hybridization. The domains of chick *Raldh2* (red) and chick *Gata4* (blue) converged in the lateral mesoderm at the level of Hensen's node contacting posterior cardiac precursors with mesoderm producing RALDH2. (D) HH8 chick RALDH2 expression starts at the lateral mesoderm from the level of the transition between the last formed somite and the unsegmented paraxial mesoderm, almost up to the anterior intestinal portal (AIP) (star). (E) HH8 chick GATA4 expression is in the lateral mesoderm from the level of somite 2 almost up to the AIP. (F,G) Chick *Raldh2* and chick *Gata4* expression in sections respectively cut from embryos in D and E at the level indicated by the upper bar. (H,I) Chick *Raldh2* and chick *Gata4* expression in sections respectively cut from embryos in D and E at the level indicated by the lower bar. Below the AIP chick *Raldh2* is expressed in splanchnic and somatic mesoderm (F). Chick *Gata4* is expressed in splanchnic mesoderm and endoderm (G). At the level of somite 2 chick *Raldh2* is expressed in mesoderm (H). Chick *Gata4* is expressed in mesoderm (I). Isotopic (35 S) in situ hybridization for RALDH2 (J) and GATA4 (K) in consecutive sections indicate that these genes are co-expressed in the splanchnic mesoderm. Ant Limit, anterior limit; e, endoderm; m, mesoderm; Post Limit, posterior limit; SOM, somatic mesoderm; SPM, splanchnic mesoderm.

The changing relationship between RALDH2 and cardiac precursors was directly established in the mouse embryo by RALDH2/Tbx-5 double in situ hybridization. At early stages, mouse *Gata4* and mouse *Tbx5* displayed similar patterns of expression and included more posterior cardiac precursors than mouse *nkx-2.5*. The mouse *Tbx5* probe gave stronger signals than mouse *Gata4* and was chosen as the marker of cardiac cells (not shown). Fig. 5 depicts embryos at stages ranging from the late allantoic bud to the 6 somite stage. At late bud stage RALDH2 was expressed exclusively in the mesoderm caudal to the node, whereas cardiac precursors were concentrated at the anterior tip of the mesoderm (Fig. 5A). In more developed late bud embryos and in embryos at the early headfold stage (Fig. 5B,C), mouse *Raldh2* expression in the lateral mesoderm expanded anteriorly towards the posterior margin of the cardiac field. Mouse *Tbx5*

expression was also increased, forming a stripe oriented in a posterior-lateral direction towards the tip of the advancing wave of RALDH2 (Fig. 5B-D). At late headfold stage, *Raldh2* and *Tbx5* expression domains converged to overlap in the most posterior cardiac precursors (Fig. 5E). The presence of posterior cardiac precursors in a field actively synthesizing and responding to RA was clearly shown in a double mouse Tbx-5 in situ hybridization/*lacZ* staining of a late headfold RARE*hsplacZ* RA-indicator embryo. At this stage only the posterior third of the mouse Tbx-5 stripe overlapped with the *lacZ* stain (Fig. 5F). As indicated by Fig. 5F-I, the encirclement of cardiac precursors by RALDH2 progressed steadily at 3-4 somite stages (arrows) and, eventually, the bilateral arches of RALDH2 joined at the midline over the AIP. There, they overlapped most posterior precursors as shown by RALDH2 whole-mount immunohistochemistry (Fig. 5J,K).

In summary, the patterns of cardiac AP signalling by RA are conserved between chicken and mice and include distinct phases. The first phase, between stages HH5-7 in the chicken and early bud to late headfold in the mouse, is characterized by increasing proximity between cardiac precursors and RALDH2. The second phase, between stages HH7 and HH8 in the chicken and late headfold to somite stages in the mouse, is characterized by a progressive encirclement of posterior cardiac precursors by a field of RALDH2.

Probing commitment to AP fates in the cardiac field

To correlate commitment to cardiac AP fates with the events of chick *Raldh2* expression in the lateral mesoderm, we assessed the stage at which cardiac precursors become determined to a specific AP fate. Commitment to posterior fates was tested with BMS493, a RA pan-antagonist, whereas commitment to anterior fates was tested with all-trans RA. Production of hearts with a reduced inflow compartment and an oversized ventricle after BMS493 was interpreted as evidence against determination of the posterior fate. Likewise, production of hearts with inflow dominance after RA was interpreted as evidence against determination of anterior fates. Production of normal hearts after treatments with BMS493 or RA indicated that posterior and anterior fates were already determined.

Fig. 6A,B shows cardiac phenotypes obtained after BMS493 10^{-4} M or all-trans RA 10^{-5}-10^{-4} M, respectively. As seen in Fig. 6A, BMS493 at HH4-7 inhibited development of cardiac inflow and turned the heart into an oversized ventricle. Conversely, BMS493 at HH8-9 failed to affect cardiac morphology. Likewise, treatment with RA at HH4-7, but not at HH8-9, produced hearts with clear inflow dominance displaying reduced or absent ventricular tissue. Fig. 6C indicates that reciprocal changes in inflow architecture induced by BMS493 or RA were consistent with the patterns of *Amhc1* expression, a marker for posterior cardiac cells.

Identical cardiac phenotypes were obtained with lower doses of BMS493 or RA, but with low penetrances that precluded systematic study. Nevertheless, we never detected any evidence of BMS493 toxicity because all effects we observed were similar to those of vitamin A deprivation. These results indicate that both anterior and posterior fates are determined between HH7-8.

Chick *Raldh2* expression and the cardiac fate map

To determine the relationship between cardiac AP fates and chick *Raldh2* expression we generated fate maps from embryos at HH7-8, the critical phases of commitment to AP fates. In agreement with previous reports (Redkar et al., 2001; Rosenquist and deHaan, 1966), labelling of anterior or posterior cardiac precursors with DiI was followed by appearance of the dye in ventricles or sino-atrial region (Fig.

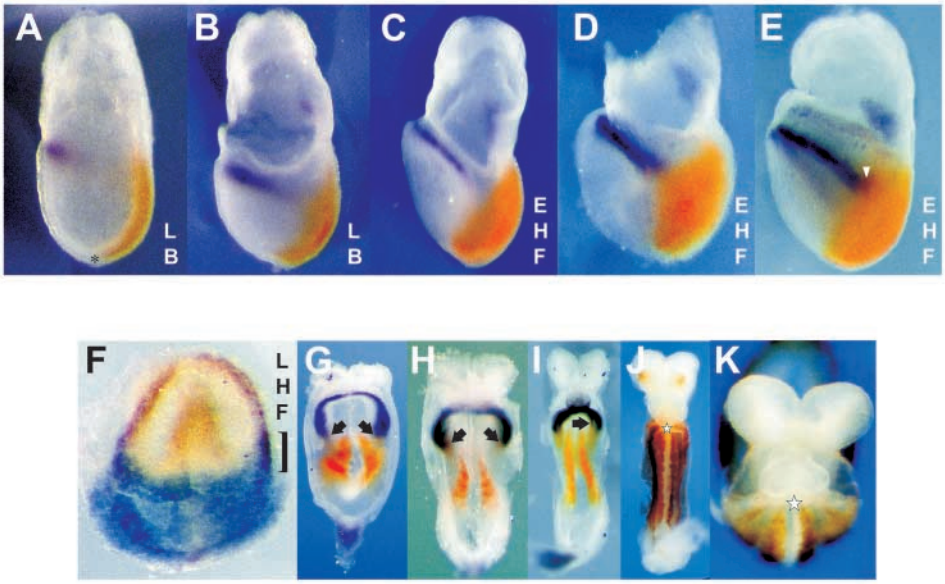

Fig. 5. Two phases of RA signalling in the mouse cardiac field. A-E (left-side views) and F-K (frontal views). A-E and G-I are mouse *Raldh2* (orange) and mouse *Tbx5* (purple) double in situ hybridizations. (A) Late bud (LB) stage. Cardiac precursors express mouse *Tbx5* and occupy an anterior position. Mouse *Raldh2* is expressed in mesoderm posterior to the node (*). Separation between cardiac precursors and RALDH2 is maximal. (B) LB stage. *Raldh2* expression expands in the anterior lateral mesoderm. Mouse *Tbx5* expression increases forming a stripe in the lateral mesoderm oriented in a posterior-direction towards the advancing RALDH2 caudorostral wave. (C) Early headfold stage (EHF). The gap separating cardiac precursors from RALDH2 is decreased. (D) EHF stage. mouse *Raldh2* expression advances to contact the most posterior cardiac precursors. (E) Late headfold stage (LHF). RALDH2 penetrates the cardiac field and overlaps posterior cardiac precursors (white arrowhead). (F) LHF stage. Double mouse Tbx-5 in situ hybridization/*lacZ* staining in RA-indicator embryos. Mouse *Raldh2* expression takes RA signalling to posterior cardiac precursors. In this embryo RA signalling overlaps the posterior third of the cardiac field (bracket). (G-I) Somite stages. Embryos display increasing overlap between *Raldh2* expression and cardiac precursors (black arrows). (J,K) RALDH2 immunohistochemistry. Arches of RALDH2 expression joined at the midline in sino-atrial tissue below the anterior intestinal portal (AIP) (star) in embryos respectively displaying looped and unlooped hearts.

7D and 7B, respectively). This was further confirmed when we superimposed grids containing information from all injection points obtained at HH7 and HH8 on appropriate embryos (Fig. 7E-H, Fig. 8B).

In Fig. 7E-H we describe the relationship between cardiac fate maps and RALDH2 expression patterns in the lateral mesoderm. To superimpose our fate maps to the RALDH2 expression domains we chose embryos that closely represented the average HH7 and HH8 patterns of chick *Raldh2* expression shown in Fig. 3C. In other words, the HH7 embryo shown in Fig. 7E has the anteriormost border of its chick *Raldh2* expression at the anterior tip of Hensen's node. Likewise, the HH8 embryo shown in Fig. 7F has an RALDH2 expression pattern in the lateral mesoderm that overlaps more than half of the cardiac field.

At HH7 there was a clear separation, centered at the mid of row E, between anterior and posterior cardiac precursors. Importantly, all but three injection sites representing posterior cardiac precursors fell within the domains of chick *Raldh2* expression. In contrast, all injection sites representing anterior cardiac precursors fell outside the domain of chick *Raldh2* expression and were separated from it by at least 100 μm (Fig. 7G).

At HH8, a significant region of overlap, centered at grid square F3, developed between anterior and posterior cardiac precursors. Nonetheless, most anterior and posterior cardiac precursors remained at their respective rostrocaudal sections in the lateral mesoderm. At this stage all injection sites representing posterior precursors were contained within the domains of chick *Raldh2* expression. Most injection sites representing anterior precursors also fell within the domains of RALDH2 such that only the rostral-most anterior precursors located at square B2 were outside the RALDH2 domain (Fig. 7H).

Thus, we demonstrated that at stage HH7, RALDH2 is present in the lateral mesoderm at a position consistent with the location of posterior, but not of anterior cardiac precursors. In contrast, at stage HH8, RALDH2 in the lateral mesoderm reaches most cardiac cells and no longer discriminates between anterior or posterior precursors.

RA signalling controls cardiac fates and is a local requirement for atrial differentiation

To establish whether RA inhibition affects specification of AP identities in the cardiac field we generated cardiac fate maps in the presence of BMS493. As shown in Fig. 8A, RA inhibition at HH7 changed the cardiac fate map. In the presence of BMS493, ventricular precursors were found in the

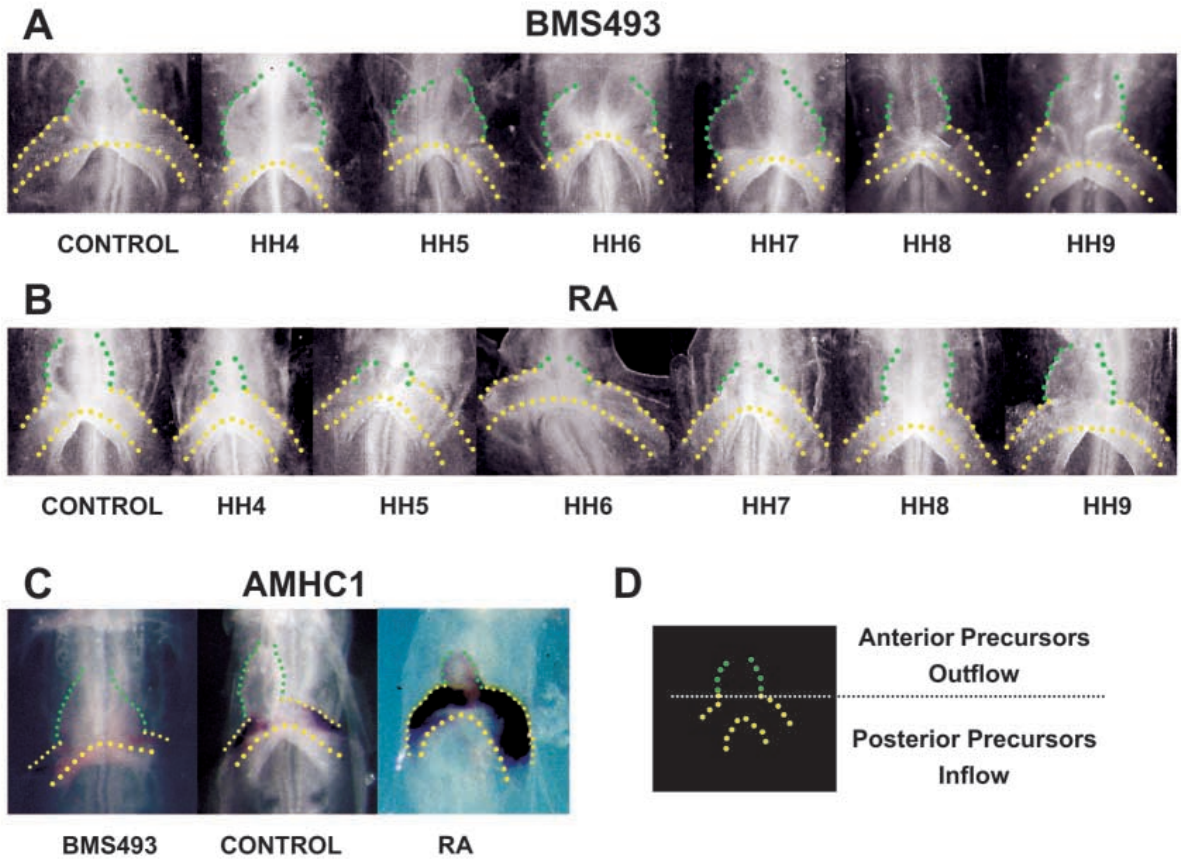

Fig. 6. Testing commitment to anteroposterior (AP) fates by reciprocal manipulation of RA signalling with RA and BMS493, a RA pan-antagonist. All pictures were taken with the same magnification. Control hearts display a central ventricular chamber flanked by bilateral limbs formed by posterior precursors. (A) BMS493 at 10^{-4} M at stages HH4-7 induced atrophy of the cardiac inflow compartment and increased the ventricular chamber. Treatment at stages beyond HH7 failed to affect cardiac morphology, indicating that posterior precursors commit to their fates between HH7-8. (B) RA at 10^{-5} to 10^{-4} M at HH4-7 inhibited ventricular development. RA treatment beyond HH7 failed to affect chamber morphology, indicating that ventricular and conotruncal precursors commit to their fates between stages HH7-8. (C) *Amhc1* expression after BMS493 and RA. (D) Codes for dots outlining cardiac structures.

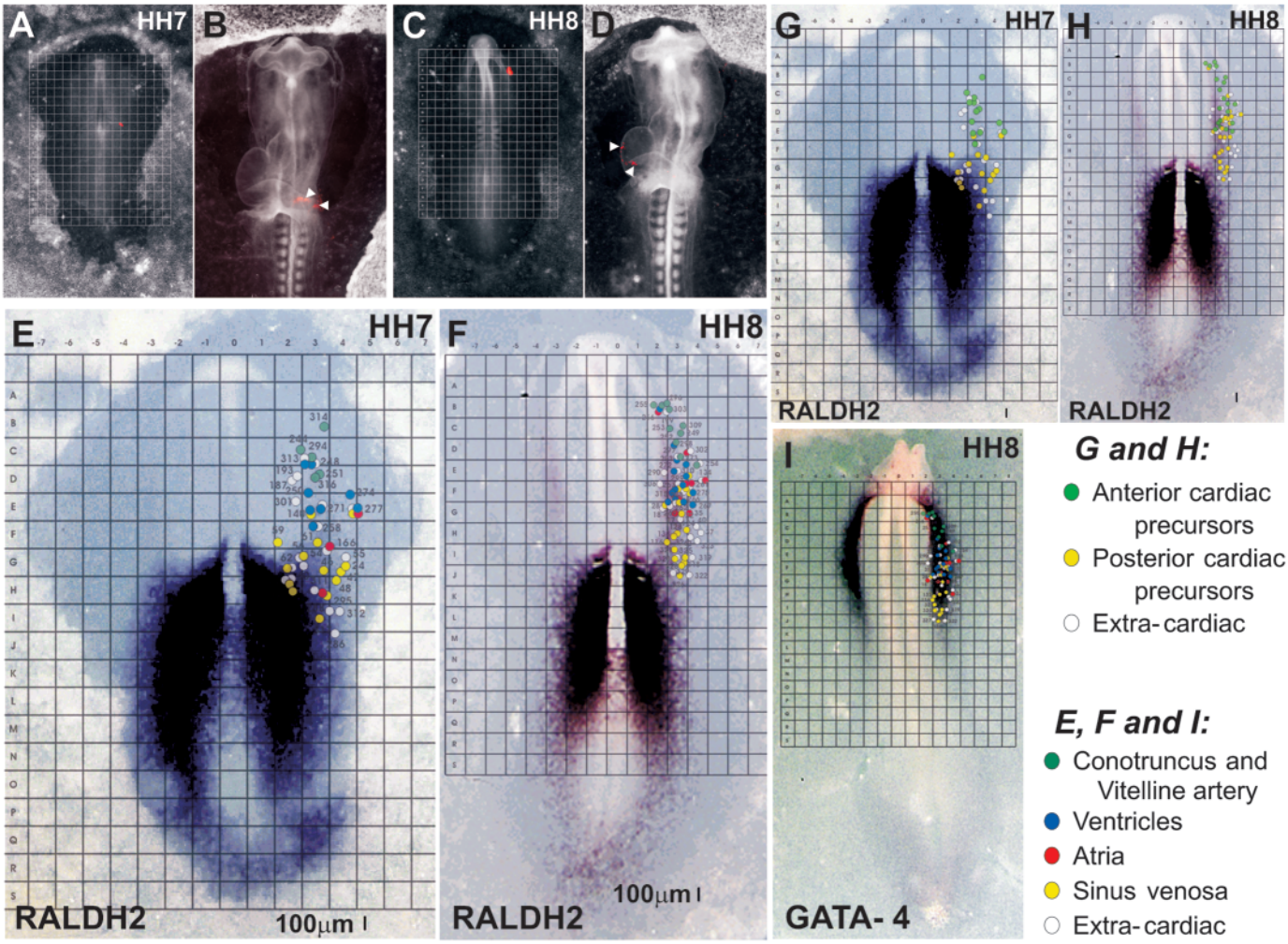

Fig. 7. The cardiac fate map and RALDH2. (A,C) Grids were superimposed on bright field/fluorescent overlays of HH7 and HH8 embryos injected with DiI in the lateral mesoderm, respectively. (B,D) Bright field/fluorescent overlays of embryos depicted in A and C at HH11^{+}, respectively. (A) DiI injected in the lateral mesoderm at the level of Hensen's node. (B) HH11^{+}. DiI injected in A was located in atrium and left sinus venosus. (C) DiI injected at the anterior lateral mesoderm. (D) HH11^{+}. DiI injected in C was located in left and right ventricles (white arrowheads). (E,F) Fate maps of embryos at stages HH7 and HH8 respectively superimposed on typical *Raldh2* expression patterns. (E) HH7. Chick *Raldh2* expression predicts the location of prospective sino-atrial precursors. (F) HH8. Anterior and posterior cardiac precursors occupy distinct territories, but chick *Raldh2* expression no longer discriminates anterior from posterior cardiac precursors. (G,H) HH7 and HH8 fate maps data grouped as anteroposterior (AP) divisions. (I) The cardiac fate map at stage HH8 was superimposed on a typical *Gata4* expression pattern.

posterior cardiac field between rows G and H, which, in the absence of treatment, contained only sino-atrial precursors (Fig. 8B). This is consistent with RA determining sino-atrial fates in posterior cardiac precursors and suggests that conversion of sino-atrial precursors to a ventricular fate is important as a mechanism of ventricular dominance after RA inhibition (Fig. 6A, Fig. 8D).

To determine the role played by local RA in the anterior lateral mesoderm we performed unilateral treatments with BMS493. Three agar cylinders containing BMS493 10^{-4} M were placed on the endoderm overlying the left lateral mesoderm between Hensen's node and headfold (Fig. 8E). As shown in Fig. 8F, RA inhibition in the left lateral mesoderm repressed expression of the atrial marker AMHC1 exclusively on the left side. This indicates that local RA signalling in the lateral mesoderm is necessary to induce atrial differentiation.

Discussion

We describe a dynamic pattern in the lateral mesoderm, a caudorostral wave of RALDH2. Using morphometric techniques we characterized the RALDH2 wave in relation to embryonic stages and to the position of the cardiac field. We demonstrate that appearance of RALDH2 in the cardiac field coincides with the critical period for cardiac AP differentiation (HH7-8) and that, at stage HH7, *Raldh2* expression in the lateral mesoderm predicts the sino-atrial fate. Using treatments with a RA receptor pan-antagonist, we showed that local RA at the lateral mesoderm is a major factor establishing sino-atrial identities in posterior cardiac precursors.

Using expression of RALDH2 to understand cardiac RA signalling

Recent advances in retinoid biology made clear that the

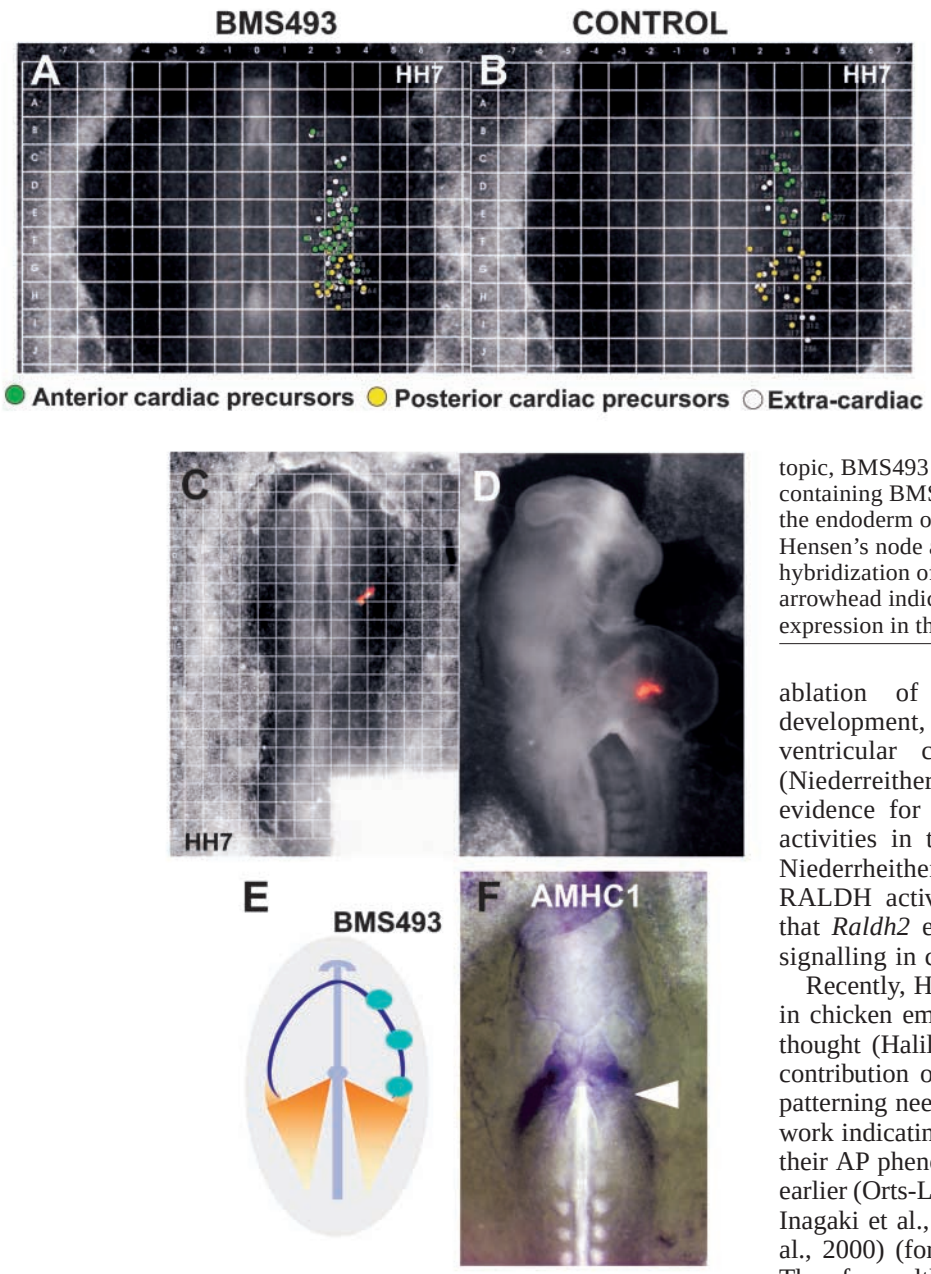

Fig. 8. RA inhibition, cardiac fate maps and *Amhc1* expression. (A) RA inhibition by BMS493 10^{-4} M changed the HH7 fate map. Anterior precursors (ventricular, conotruncal and vitelline artery) are found at posterior regions of the cardiac field which otherwise contained only sino-atrial (posterior) precursors in the absence of BMS493 (compare with B). (B) Normal HH7 fate map (same data as Fig. 7G). (C) HH7. Bright field/fluorescent overlay of a BMS493-treated embryo injected at a posterior site in the cardiac field, which is normally devoid of ventricular precursors. (D) $HH11^{+}$. Bright field/fluorescent overlay of the embryo in C. DiI is located in the ventricle. (E) Scheme of unilateral, topic, BMS493 treatment at HH6. Three agar cylinders containing BMS493 at 10^{-4} M (blue circles) were placed on the endoderm overlying the left lateral mesoderm between Hensen's node and headfold. (F) HH10. AMHC1 in situ hybridization of a BMS493-treated embryo. White arrowhead indicates unilateral inhibition of *Amhc1* expression in the left lateral mesoderm.

dynamic and elaborated patterns of RA signalling during embryogenesis require more sophisticated regulatory options than those provided by RA receptors and their patterns of expression. In short time, work on RALDHs and RA-degrading enzymes have confirmed that retinoid signalling cannot be understood without knowing how these enzymes are regulated (Duester et al., 2003; Swindell et al., 1999).

Amongst the RALDHs, RALDH2 is the first expressed and its appearance coincides with initiation of RA synthesis in the mouse embryo (Ulven et al., 2000). Furthermore, *Raldh2* expression coincides with the response to endogenous RA in hearts from immediately after fusion of cardiac primordia, up to looping and wedging stages (Moss et al., 1998). In this study we extend these findings to show that *Raldh2* expression faithfully represents RA signalling in cardiac precursors even before their fusion (Fig. 5E,F). In addition, ablation of the *Raldh2* gene abrogates atrial development, promotes premature differentiation of ventricular cells and leads to embryonic death (Niederreither et al., 2001). Thus, although there is evidence for novel, as yet uncharacterized, RALDH activities in the developing heart (Mic et al., 2002; Niederrheither et al., 2002), RALDH2 is a major RALDH activity in cardiac development, suggesting that *Raldh2* expression is an accurate readout of RA signalling in cardiac precursors.

Recently, Halilagic et al. indicated that RA signalling in chicken embryos starts much earlier than previously thought (Halilagic et al., 2003). However, the putative contribution of this early RA signalling to cardiac AP patterning needs to be evaluated in the light of previous work indicating that cardiac cells commit irreversibly to their AP phenotypes between stages HH7 and 8, but not earlier (Orts-Llorca and Collado, 1967; Satin et al., 1988; Inagaki et al., 1993; Yutzey et al., 1995; Patwardhan et al., 2000) (for a review, see Xavier-Neto et al., 2001). Therefore, although earlier RA signalling by enzymes other than RALDH2 may play a major role in cardiac development and be necessary or permissive for induction of RALDH2 in the appropriate regions of the cardiogenic plate, the data available indicate that the crucial decision between anterior or posterior fates occurs at developmental times when RALDH2 is the only RALDH enzyme expressed in a clear AP pattern in the cardiac mesoderm.

GATA4 as a marker for the early cardiac field

In this study we utilized GATA4 instead of Nkx-2.5 as a marker for the cardiac field. This choice was validated by comparing our cardiac fate maps with typical in situ hybridization patterns for GATA4. As shown in Fig. 7I, the GATA4 expression domain matched the distribution of the cardiac field at stage HH8. This observation is consistent with previous studies showing that GATA4 is highly expressed in the lateral mesoderm from the level of the AIP to somite 3 (Jiang et al.,

1998; Kostetskii et al., 1999) (Fig. 4F), a domain which encompasses all cardiac precursors as determined by our fate map in Fig. 7I or almost all cardiac precursors according to a previous fate map study (Redkar et al., 2001). In contrast, in agreement with the study of Redkar et al. (Redkar et al., 2001), the Nkx-2.5 domain fell short of labelling all cardiac precursors, leaving behind the caudal third of the cardiac field where sino-atrial precursors predominate (data not shown). Thus, our data indicate that GATA4 is a better marker for the early cardiac field than Nkx-2.5.

The patterns of *Raldh2* expression are consistent with roles for RA in specification and determination of cardiac AP fates

We showed that *Raldh2* expression and RA signalling were confined to mouse sino-atrial tissues from 8.25 to 9.5 dpc (Moss et al., 1998). Using chicken embryos we demonstrated that atrial precursors co-expressed *Amhc1* and chick *Raldh2* as early as stage 9⁻, indicating that the association between atrial precursors and RALDH2 could be pushed further back in time (Xavier-Neto et al., 2000). Although these observations were consistent with a role of RA in the maintenance and development of the sino-atrial phenotype, they were not sufficient to prove that an endogenous RA signal was a determinant factor at the earlier developmental periods when the sino-atrial fate is determined. Therefore, this study was performed to fill the gap in our knowledge of the relationship between RALDH2 and the cardiac field at the critical stages of AP differentiation.

The progressive adherence of cardiac precursors to their AP phenotypes has been studied. Using different techniques, several investigators established that cardiac AP fates are specified between HH4-7 and determined around HH7-8 (Orts Llorca and Collado, 1967; Satin et al., 1988; Inagaki et al., 1993; Yutzey et al., 1995; Patwardhan et al., 2000). We extend these findings by showing, through reciprocal manipulations of RA signalling, that cardiac AP fates remain plastic from HH4-7, but not after HH8.

We describe two phases of the dynamic relationship between *Raldh2* expression and cardiac precursors that fit into the paradigms of specification and determination. In the chick embryo Phase 1 spans stages HH4-7, and is characterized by progressive closure of a spatial gap that separates RALDH2 from the cardiac field (Fig. 3C, Fig. 4). The patterns of *Raldh2* expression during Phase 1 suggest that RA concentrations reaching the posterior cardiac field increase gradually from low values at stage HH4-5 to higher values at HH7, as the distance between source and target tissue decrease. Such profile of increasing RA concentrations in posterior cardiac precursors would be consistent with the pattern of increasing association of these cells to the sino-atrial phenotype. As shown by Yutzey et al. only 67% of explants containing posterior cardiac cells at stage HH5-6 expressed *Amhc1* after 2 days of culture (Yutzey et al., 1995). In contrast, 95% of posterior explants at stage HH7-8 expressed *Amhc1*, indicating a stronger adherence of posterior cardiac cells to the sino-atrial phenotype. However, cardiac AP fates are not determined even at HH7 (Fig. 6). In fact, posterior cardiac precursors commit irreversibly to their sino-atrial fates only between HH7-8 when *Raldh2* expression is at Phase 2 and invading the cardiac field. Therefore, the patterns of *Raldh2* expression at Phase 2 suggest that RA concentrations reaching prospective sino-atrial precursors would attain a maximal value when RALDH2 encircles these cells, eliminating the distance between source and target tissue (Fig. 4J,K). Thus, at Phase 2, direct exposure of the posterior cardiac field to high concentrations of RA produced in situ would be consistent with an irreversible attainment of sino-atrial identity. In summary, our data indicate that *Raldh2* expression is present at the right times and places to direct both specification and determination inside each AP domain. It is probable, however, that fate determination at the cardiac AP boundary is more complex than inside each AP domain. At stage HH7 we detected a very limited degree of overlap between anterior and posterior cardiac fields (Fig. 7E). Although this may reflect an intrinsic limitation of fate mapping techniques, which cannot offer more than an approximate view of dynamic events, fate determination at the AP boundary will probably involve an interplay of position, movement as well as extent and timing of exposure to RA signalling.

Is anterior the myocardial default?

Because RA signalling is required in the posterior cardiac field to induce the sino-atrial phenotype in cells that would otherwise differentiate into anterior cell types (Fig. 8), it is tempting to speculate that the default fate of the myocardium is an undifferentiated anterior cell. Evidence from RA-insufficiency studies supports this notion (Heine et al., 1985; Niederreither et al., 1999; Chazaud et al., 1999; Xavier-Neto et al., 1999). Moreover, several morphogens induce ectopic cardiac tissue expressing *vmhc1*, but not the atrial marker *Amhc1* (Lopez-Sanchez et al., 2002). This is reminiscent of the patterns of AP patterning in caudal hindbrain, where RA is required to specify rhombomeres (r) 5-8 acting on a tissue whose default is r4 (Dupé and Lumsden, 2001). In fact, cardiac AP differentiation parallels caudal hindbrain patterning. It is even probable that the somitic mesoderm constitutes a shared source of RA for AP specification of heart and hindbrain. Although somites may provide all the RA required for hindbrain patterning, our data suggest that a new strategy evolved in the form of a caudorostral wave of RALDH2 to provide the RA concentrations that pattern cardiac precursors in the AP axis. Experience with other systems, however, suggests that a double assurance mechanism may operate in cardiac AP patterning, such that there may be separate determinants for each cardiac AP fate. Whatever is the identity of the putative anterior cardiac inducer it is clear that its actions must be recessive to the posteriorizing RA signal.

The fate of cardiac precursors after manipulations of RA signalling

Inhibition of RA signalling by BMS493 repressed AMHC1 expression and produced hearts with ventricular dominance, whereas RA increased AMHC1 expression and produced hearts with inflow dominance (Fig. 6). Inflow/outflow dominance after manipulation of RA signalling could be caused by multiple mechanisms such as conversion between atrial and ventricular phenotypes, selective proliferation or apoptosis. In Fig. 8 we showed, in a fate map performed under BMS493, that ventricular precursors were found in regions of the cardiac field, which, in the absence of treatment, contained only sino-atrial precursors. This suggests that atrial precursors converted to ventricular phenotypes in the absence of RA

signalling. Conversely, previous studies by Yutzey et al. showed that exogenous RA increased the domain of AMHC1 without interfering with VMHC1 expression or heart size and induced AMHC1 expression in ventricular precursors (Yutzey et al., 1994; Yutzey et al., 1995). These experiments suggested that increased RA signalling converted ventricular precursors into atrial cells. Moreover, we showed in transgenic mice that exogenous RA induced expression of the atrial-specific marker SMyHC3-HAP in cells that already expressed MLC2-V, a ventricular-specific marker (Xavier-Neto et al., 1999). This experiment provided direct in vivo evidence that exogenous RA can induce an atrial program in ventricular cells.

Thus, although our experiments here were not designed to address specifically the fates of cardiac precursors after manipulations of RA signalling, data in this manuscript as well as in previous studies support a role for conversion between atrial and ventricular phenotypes in cardiac chamber dominance. Alternative possibilities include: cell-cycle withdrawal, apoptosis, delayed AP differentiation or switch to a non-cardiac fate. A quantitative assessment of the role played by these mechanisms is not yet available. However, it is unlikely that atrial precursors exposed to BMS493 would take on mesodermal fates other than the cardiac, because at the stage when we performed these experiments (HH6) cardiac precursors are already determined as such (Montgomery et al., 1994). Therefore, although multiple mechanisms can contribute to cardiac chamber dominance after changes in RA status, the evidence strongly indicates that conversion between atrial and ventricular does play a role in this process.

Role of RA signalling after determination of AP fates

RALDH2-null embryos display an abnormal ventricular phenotype as early as 8.5 dpc, suggesting a role for RALDH2 in ventricles at this stage (Niederreither et al., 2001). However, at this time no mouse *Raldh2* expression can be detected in wild-type ventricles (Moss et al., 1998). Moreover, although RA diffuses to several hundred micrometers (Eichele and Thaller, 1987), there is no evidence, before 12.5 dpc, for an endogenous RA response in the ventricles of RA-indicator embryos (Moss et al., 1998).

Our results suggest an explanation for this apparent paradox. In the chick embryo, stages HH8-10 constitute a previously undetected window for transient expression of the chick *Raldh2* gene in ventricular precursors before fusion of cardiac primordia (Fig. 1, Fig. 3C, Fig. 7). Because cardiac AP fates are already determined at HH8 (Fig. 6), exposure of anterior cardiac precursors to RA at HH8-9 must serve a developmental program distinct from AP patterning. Expression of *Raldh2* in ventricular precursors prior to fusion of cardiac primordia may activate RA-dependent pathways later in chicken ventricles. It remains to be established by fate-mapping whether mouse ventricular precursors also express *Raldh2* before cardiac fusion. If this proves to be the case, the RALDH2 caudorostral wave may constitute the long sought non-epicardial source of RA inhibiting precocious differentiation and maintaining proliferation in mouse 8.5 to 9.5 dpc ventricles (Kastner et al., 1997).

RALDH2 and cardiac AP differentiation: updating the model

A few years ago we proposed a model for cardiac AP patterning based on selective signalling by RA (Rosenthal and Xavier-Neto, 2000; Xavier-Neto et al., 2001). According to the model, RA signalling in posterior cardiac precursors determines the sino-atrial fate, whereas absence of it determines ventricular and conotruncal fates. Our data support the model as proposed initially and also refine it. New findings include description of tissue sources of RA for cardiac AP patterning and evidence for active roles of cardiac precursors in the interpretation of RA concentrations. Paraxial and lateral mesoderm are probable sources of RA for the specification of sino-atrial identities, whereas RA in the anterior lateral mesoderm is critical for expression of *Amhc1* and determination of the sino-atrial fate. Our results suggest that cardiac precursors must read RA concentrations in a stage-dependent fashion. In fact, at stage HH7, anterior cardiac precursors at the edge of RALDH2 expression must be exposed to RA concentrations much higher than the ones experienced by posterior precursors at earlier stages (Fig. 7E), and yet they do not differentiate in sino-atrial cells, indicating that there is no single RA threshold that will, at all times, push a given cardiac precursor towards a sino-atrial fate.

In summary, our results are consistent with a two-step model of cardiac AP patterning. First, posterior cardiac precursors are specified to a sino-atrial fate by low concentrations of RA reaching the posterior cardiac field through diffusion from lateral and paraxial mesoderm. Later, posterior cardiac precursors commit irreversibly to a sino-atrial fate in response to increased concentrations of RA produced by the caudorostral wave of RALDH2.

We are indebted to Bristol Myers Squibb for BMS493. This work was supported by grants from FAPESP (01/00009-0, 00/14454-3, 02/13652-1), CNPq (478843/01-1) and CAPES.

References

Bruneau, B. G. (2002). Transcriptional regulation of vertebrate cardiac morphogenesis. *Circ. Res.* **90**, 509-519.

Bruneau, B. G., Logan, M., Davis, N., Levi, T., Tabin, C. J., Seidman, J. G. and Seidman, C. E. (1999). Chamber-specific cardiac expression of *Tbx5* and heart defects in Holt-Oram syndrome. *Dev. Biol.* **211**, 100-108.

Cardoso, W. V., Mitsialis, S. A., Brody, J. S. and Williams, M. C. (1996). Retinoic acid alters the expression of pattern-related genes in the developing rat lung. *Dev. Dyn.* **207**, 47-59.

Chapman, S. C., Collignon, J., Schoenwolf, G. C. and Lumsden, A. (2001). Improved method for chick whole-embryo culture using a filter paper carrier. *Dev. Dyn.* **220**, 284-289.

Chazaud, C., Chambon, P. and Dollé, P. (1999). Retinoic acid is required in the mouse embryo for left-right asymmetry determination and heart morphogenesis. *Development* **126**, 2589-2596.

De Jong, F., Opthof, T., Wilde, A. A. M., Janse, M. J., Charles, R., Lamers, W. H. and Moorman, A. F. M. (1992). Persisting zones of slow impulse conduction in developing chicken hearts. *Circ. Res.* **71**, 240-250.

Downs, K. M. and Davies, T. (1993). Staging of gastrulating mouse embryos by morphological landmarks in the dissecting microscope. *Development* **118**, 1255-1266.

Duester, G., Mic, F. A. and Molotkov, A. (2003). Cytosolic retinoid dehydrogenases govern ubiquitous metabolism of retinol to retinaldehyde followed by tissue-specific metabolism to retinoic acid. *Chem. Biol. Interact.* **144**, 201-210.

Dupé, V. and Lumsden, A. (2001). Hindbrain patterning involves graded responses to retinoic acid signalling. *Development* **128**, 2199-2208.

Eichele, G. and Thaller, C. (1987). Characterization of concentration gradients of a morphogenetically active retinoid in the chick limb bud. *J. Cell Biol.* **105**, 1917-1923.

Garcia-Martinez, V. and Schoenwolf, G. C. (1993). Primitive streak origin of the cardiovascular system in avian embryo. *Dev. Biol.* **159**, 706-719.

Halilagic, A., Zile, M. H. and Studer, M. (2003). A novel role for retinoids in patterning the avian forebrain during presomite stages. *Development* **130**, 2039-2050.

Hamburger, V. and Hamilton, H. L. (1951). A series of normal stages in the development of the chick embryo. *J. Morph.* **88**, 49-92.

Heine, U. I., Roberts, A. B., Munoz, E. F., Roche, N. S. and Sporn, M. B. (1985). Effects of retinoic deficiency on the development of the heart and vascular system of the quail embryo. *Virchows. Arch.* **50**, 135-152.

Houzelstein, D. and Tajbakhsh, S. (1999). Increased in situ hybridization sensitivity using non-radioactive probes after staining for galactosidase activity. *Tech. Tips Online*.

Inagaki, T., Garcia-Martinez, V. and Schoenwolf, G. C. (1993). Regulative ability of the prospective cardiogenic and vasculogenic areas of the primitive streak during avian gastrulation. *Dev. Dyn.* **197**, 57-68.

Jiang, Y., Tarzami, S., Burch, J. B. and Evans, T. (1998). Common role for each of the cGATA-4/5/6 genes in the regulation of cardiac morphogenesis. *Dev. Genet.* **22**, 263-277.

Kastner, P., Messaddeq, N., Mark, M., Wendling, O., Grondona, J. M., Ward, S., Ghyselinck, N. and Chambon, P. (1997). Vitamin A deficiency and mutations of RXRalpha, RXRbeta and RARalpha lead to early differentiation of embryonic ventricular cardiomyocytes. *Development* **124**, 4749-4758.

Kostetskii, I., Jiang, Y., Kostetskaia, E., Yuan, S., Evans, T. and Zile, M. (1999). Retinoid signalling required for normal heart development regulates GATA-4 in a pathway distinct from cardiomyocyte differentiation. *Dev. Biol.* **206**, 206-218.

Lopez-Sanchez, C., Climent, V., Schoenwolf, G. C., Alvarez, I. S. and Garcia-Martinez, V. (2002). Induction of cardiogenesis by Hensen's node and fibroblast growth factors. *Cell Tissue Res.* **309**, 237-249.

Mic, F. A., Haselbeck, R. J., Cuenca, A. E. and Duester, G. (2002). Novel retinoic acid generating activities in the neural tube and heart identified by condicional rescue of *Raldh2* null mutant mice. *Development* **129**, 2271-2282.

Molotkov, A., Fan, X., Deltour, L., Foglio, M. H., Martras, S., Farrés, J., Parés, X. and Duester, G. (2002). Stimulation of retinoic acid production and growth by ubiquitously-expressed alcohol dehydrogenase *Adh3*. *Proc. Natl. Acad. Sci. USA* **99**, 5337-5342.

Montgomery, M. O., Litvin, J., Gonzalez-Sanchez, A. and Bader, D. (1994). Staging of commitment and differentiation of avian cardiacmyocytes. *Dev. Biol.* **164**, 63-71.

Moss, J. B., Xavier-Neto, J., Shapiro, M. D., Nayeem, S. M., McCaffery, P., Dräger, U. C. and Rosenthal, N. (1998). Dynamic patterns of retinoic acid synthesis and response in the developing mammalian heart. *Dev. Biol.* **199**, 55-71.

Niederreither, K., Subbarayan, V., Dollé, P. and Chambon, P. (1999). Embryonic retinoic acid synthesis is essential for early mouse post-implantation development. *Nat. Genet.* **21**, 444-448.

Niederreither, K., Vermot, J., Messaddeq, N., Schuhbaur, B., Chambon, P. and Dollé, P. (2001). Embryonic retinoic acid synthesis is essential for heart morphogenesis in the mouse. *Development* **128**, 1019-1031.

Niederreither, K., Vermot, J., Fraulob, V., Chambon, P. and Dollé, P. (2002). Retinaldehyde dehydrogenase 2 (RALDH2)-independent patterns of retinoic acid synthesis in the mouse embryo. *Proc. Natl. Acad. Sci. USA* **99**, 16111-16116.

Orts-Llorca, F. and Jimenez Collado, J. (1967). Determination of heart polarity (arterio-venous axis) in the chicken embryo. *Roux's Arch. EntwMech. Org.* **158**, 146-163.

Patwardhan, V., Fernandez, S., Montgomery, M. and Litvin, J. (2000). The rostro-caudal position of cardiac myocytes affects their fate. *Dev. Dyn.* **218**, 123-135.

Pérez-Pomares, J. M., Phelps, A., Sedmerova, M., Carmona, R., González-Iriarte, M., Muñoz-Chápuli, R. and Wessels, A. (2002). Experimental studies on the spatiotemporal expression of WT1 and RALDH2 in the embryonic avian heart: a model for the regulation of myocardial and valvuloseptal development by epicardially derived cells (EPDCs). *Dev. Biol.* **247**, 307-326.

Redkar, A., Montgomery, M. and Litvin, J. (2001). Fate map of early avian cardiac progenitor cells. *Development* **128**, 2269-2279.

Rosenquist, G. C. and deHaan, R. L. (1966). Migration of precardiac cells in the chick embryo: a radioautographic study. *Carnegie Inst. Washington Publ*. 625 (Contrib to Embryol) **38**, 111-121.

Rosenthal, N. and Xavier-Neto, J. (2000). From the bottom of the heart: anteroposterior decisions in cardian muscle differentiation. *Curr. Opin. Cell Biol.* **12**, 742-746.

Rossant, J., Zirngibl, R., Cado, D., Shago, M. and Giguère, V. (1991). Expression of a retinoic acid response element-*hsplacZ* transgene defines specific domains of transcriptional activity during mouse embryogenesis. *Genes Dev.* **5**, 1333-1344.

Rugh, R. (1952). *Experimental Embryology: A Manual of Techniques and Procedures*. Minneapolis, MN, USA: Burgess Publishing Company.

Sassoon, D. and Rosenthal, N. (1993). Detection of messenger RNA by in situ hybridization. *Methods Enzymol.* **255**, 384-404.

Satin, J., Fujii, S. and DeHaan, R. L. (1988). Development of cardiac beat rate in early chick embryos is regulated by regional cues. *Dev. Biol.* **129**, 103-113.

Stern, C. D. (1998). Detection of multiple gene products simultaneously by in situ hybridization and immunohistochemistry in whole mounts of avian embryos. *Curr. Top. Dev. Biol.* **36**, 223-243.

Streit, A. (2002). Extensive cell movements accompany formation of the otic placode. *Dev. Biol.* **249**, 237-254.

Stuckmann, I., Evans, S. and Lassar, A. B. (2003). Erythropoietin and retinoic acid, secreted from the epicardium, are required for cardiac myocyte proliferation. *Dev. Biol.* **255**, 334-349.

Swindell, E. C., Thaller, C., Sockanathan, S., Petkovich, M., Jessell, T. M. and Eichele, G. (1999). Complementary domains of retinoic acid production and degradation in the early chick embryo. *Dev. Biol.* **216**, 282-296.

Ulven, S. M., Gundersen, T. E., Weedon, M. S., Landaas, V. O., Sakhi, A. K., Fromm, S. H., Geronimo, B. A., Moskaug, J. O. and Blomhoff, R. (2000). Identification of endogenous retinoids, enzymes, binding proteins, and receptors during early postimplantation development in mouse: important role of retinal dehydrogenase type 2 in synthesis of all-*trans*-retinoic acid. *Dev. Biol.* **220**, 379-391.

Wilkinson, D. G. (1992). Whole mount in situ hybridization of vertebrate embryos. In *In Situ Hybridization: A Practical Approach* (ed. D. G. Wilkinson), pp. 75-83. Oxford, UK: IRL Press.

Xavier-Neto, J., Neville, C. M., Shapiro, M. D., Houghton, L., Wang, G. F., Nikovits, W., Jr, Stockdale, F. E. and Rosenthal, N. (1999). A retinoic acid-inducible transgenic marker of sino-atrial development in the mouse heart. *Development* **126**, 2677-2687.

Xavier-Neto, J., Shapiro, M. D., Houghton, L. and Rosenthal, N. (2000). Sequential programs of retinoic acid synthesis in the myocardial and epicardial layers of the developing avian heart. *Dev. Biol.* **219**, 129-141.

Xavier-Neto, J., Rosenthal, N., Silva, F. A., Matos, T. G., Hochgreb, T. and Linhares, V. L. (2001). Retinoid signalling and cardiac anteroposterior segmentation. *Genesis* **31**, 97-104.

Yutzey, K. E., Rhee, J. T. and Bader, D. (1994). Expression of the atrial-specific myosin heavy chain AMHC1 and the establishment of anteroposterior polarity in the developing chicken heart. *Development* **120**, 871-883.

Yutzey, K. E., Gannon M. and Bader, D. (1995). Diversification of cardiomyogenic cell lineages in vitro. *Dev. Biol.* **170**, 531-541.

Zhao, D., McCaffery, P., Ivins, K. J., Neve, R. L., Hogan, P., Chin, W. W. and Dräger, U. C. (1996). Molecular identification of a major retinoic acid synthesizing enzyme, a retinaldehyde dehydrogenase. *Eur. J. Biochem.* **15**, 15-22.

Table S1. Sites of DiI injection at HH7 and location at HH11^{+}

Embryo number	Grid code at HH7	Location at HH11+
24	G4	SV
46	G3	SV
47	G4	SV
48	H4	SV
54	G2/3	SV
55	G4	SV
56	G2/3	SV and notochord
58	H2	SV and LM
59	F2	SV
60	H2	LM
61	F3	SV
62	G2	SV and LM
140	E3	SV and V
166	F/G3	A and AP
187	D2	HM
193	D2	HM
244	C2	VA
248	C3	V, P and AP
250	D/E3	VA
251	D3	VA
258	F3	V and AP
271	E3	V and AP
274	E4	V
277	E4	SV, A, V and AP
282	H2	SV
286	J4	AP
288	I3/4	LM
294	C3	VA
295	H3	SV and A
301	E2	AP
311	H3	LM
312	I4	LM
313	C3	V, HM and AP
314	B3	CT
316	D3	CT
317	I3	SV

SV, sinus venosa; A, atria; V, ventricles; CT, conotruncus; VA, vitelline artery; HM, head mesoderm; LM, lateral mesoderm; AP, area pellucida.

Table S2. Sites of DiI injection at HH8 and location at HH11^{+}

Embryo number	Grid code at HH8	Location at HH 11+
17	G3	A
18	G2	A and AP
23	G3	LM
28	G2	SV
32	H3	SV
35	G4	A
37	H4	A
40	H4	AP
42	H4	AP
116	H2	SV
124	H3/4	SV
128	G3	AP
133	H3	SV
134	E/F4	A and AP
199	B2	HM
249	C3	VA
252	D3	V and VA
253	C3	CT
254	E4	CT, P and AP
255	B2	CT
256	B2	A, V and CT
261	F4	A and AP
262	F/G3	SV, A, V and HM
263	F3	SV and V
266	F/G3	V
267	G4	V
268	F3	SV, A, V and HM
269	G3	AP
272	E3	V and AP
273	E3	V
275	F4	SV and V
290	E2	HM
292	D/E3	V
296	B2/3	CT
297	D3	CT and HM
298	D3	A
299	F3	AP
302	D4	AP
303	B3	CT
306	F2	HM
309	C3	CT
310	E3/4	SV and V
315	F3	V
318	I3	SV
319	I4	LM
320	I3	SV
321	I3	SV
322	J4	LM
323	H4	AP
325	I3	SV
326	J3	SV
327	J3	AP
328	I3	LM
329	I/J3	SV

SV, sinus venosa; A, atria; V, ventricles; CT, conotruncus; VA, vitelline artery; HM, head mesoderm; LM, lateral mesoderm; AP, area pellucida.

Table S3. Fate map in the presence of BMS493 10^{-4} M:Sites of DiI injection at HH7 and location at HH11^{+}

Embryo number	Grid code at HH7	Location at HH11+
13	G3	A and V
14	F3	V
15	E2	HM and AP
16	F2	V
17	F2/3	V and HM
18	F2	V and HM
19	F3	V and HM
21	F3	AP and AIP
22	G3	SV
23	F2	V and AP
24	F3	V and HM
25	F3	V and AP
29	G/H3	A and V
30	G3	VA and AP
31	E3	VA and HM
32	F3	HM
33	F2	V
34	G3	AP
35	F3	A and V
37	F3	AP
38	F3	SV and V
39	F3	V and HM
41	F3	V
43	G3	SV
45	G3	SV
48	F3	HM
49	H2	SV, A and AP
50	H3	AP
52	H3	HM
54	H3	A and AP
55	H2	SV
56	G3	V and HM
57	G/H4	AP
58	G3/4	HM
59	G4	V and AP
60	H3	A and P
61	G3	HM
64	H4	SV and AP
65	H3	V
66	H3	SV
67	D3	AP
68	E4	CT and AP
69	D3	HM
71	E3	V and HM
73	C3	AP
74	E3	AP
76	E3	VA and HM
77	E3	HM
78	E3	CT
79	E3	HM
80	D3	HM
81	E3	CT and HM
82	B2	CT, HM and AP
84	D3	AP
85	D3	VA
86	C3	AP
87	C3	CT and VA

SV, sinus venosa; A, atria; V, ventricles; CT, conotruncus; VA, vitelline artery; HM, head mesoderm; LM, lateral mesoderm; AP, area pellucida.